Journal of Alloys and Compounds 509 (2011) 2243–2247

Contents lists available at ScienceDirect

Journal of Alloys and Compounds

journal homepage: www.elsevier.com/locate/jallcom

Strengthening mechanisms in particulate Al/B_4C composites produced by repeated roll bonding process

Morteza Alizadeh*

Department of Materials Science and Engineering, Shiraz University of Technology, Modarres Blvd., 3619995161, Shiraz, Iran

ARTICLE INFO

Article history:
Received 3 August 2010
Received in revised form 24 October 2010
Accepted 1 November 2010
Available online 9 November 2010

Keywords:
Metal–matrix composites
Mechanical properties
Microstructure

ABSTRACT

In this study, aluminum metal matrix composites reinforced with 5 and 10 vol.% B_4C particulates were fabricated by repeated roll bonding process. The microstructure of the composites, evaluated by optical microscopy, showed the B_4C particles are properly distributed in the aluminum matrix. A combined microstructure strengthening analysis suggested by Sekine and Chen was used to predict the yield strength of the Al/B_4C composites. In addition, the yield strength of the composites was determined by tensile tests and compared with the calculated yield strength. The results indicated that there is a good agreement between the calculated yield strength and experimental value.

1. Introduction

Particle-reinforced aluminum metal matrix composites (Al MMCs) are being considered as a group of new advanced materials due to lightweight, high strength, high specific modulus, low coefficient of thermal expansion and good wear resistance [1,2]. The strength of these materials is predictable by some methods. Several researchers have developed some theoretical prediction methods to describe the strength of whisker and particle-reinforced MMCs [3–5]. The shear lag model [5] was developed to predict the strength of composites, but it is not appropriate when the reinforcing phase possesses a small aspect ratio. The yield strength of discontinuous aligned fiber-reinforced MMCs can be predicted by the shear lag theory as follows [5]:

$$\sigma_{cy} = \sigma_{my}\left(\frac{V_f S}{2} + V_m\right) \quad (1)$$

where σ_{cy} and σ_{my} are the yield strengths of the composite and matrix respectively, V_f and V_m denote the fiber and matrix volume fractions respectively and S is the mean aspect ratio. For particle-reinforced composites, S is smaller than two. As a result, the yield strength of the composite σ_{cy} is smaller than the yield strength of the matrix σ_{my}, based on Eq. (1), which is strange for real composites. Nardone and Prewo [6] considered the transfer of tensile load at the fiber ends to modify the shear lag theory as follows:

$$\sigma_{cy} = \sigma_{my}\left[\frac{V_f(S+2)}{2} + V_m\right] \quad (2)$$

The theoretical prediction by means of this model is closer to the experimental results when the aspect ratio is small. An 'engineering' approximation on the basis of the shear lag model could be better than other theories in predicting the yield strength of composites [7]. However, the theory based on the shear lag model tends to underestimate the yield strength of composites when the matrix alloys are originally low strength aluminum alloys, such as pure and cast aluminum alloys.

The strength of particle-reinforced MMCs is found to be related to the volume fraction and diameter of the particles from the micromechanics approach [4]. The yield strength of particle-reinforced MMCs is much higher than the result predicted by continuum mechanics theories. This incremental increase of the yield strength is due to the much higher dislocation density and smaller subgrain size in the matrix than in the unreinforced alloy [8]. A model to predict the yield strength of a particle-reinforced MMC by considering the dislocation density due to mismatch between thermal expansion coefficients of the particle and matrix was built up, and the predicted yield strength was found to be consistent with experimental results [9]. The yield strength of composites can also be affected by thermal residual stress due to the mismatch of thermal expansion coefficients [9]. Sekine and Chen [3] suggested a combined microstructure strengthening analysis based on the modified shear lag theory to predict the yield strength of SiC particle-reinforced low strength aluminum composites as

* Corresponding author. Tel.: +98 711 7354500; fax: +98 711 7354520.
E-mail address: Alizadeh@sutech.ac.ir

0925-8388/$ – see front matter © 2010 Elsevier B.V. All rights reserved.
doi:10.1016/j.jallcom.2010.11.004

Table 1
Chemical composition of the 1100 Al alloy.

Element	Al	Si	Fe	Cu	Mn	Zn	Ti	Cr	Ni
Wt (%)	99.48	0.12	0.222	0.12	0.04	0.01	0.005	0.0016	0.0014

follows:

$$\sigma_{cy} = \sigma^*_{my}\left[\frac{V_f(S+2)}{2} + V_m\right] \quad \text{and}$$

$$\sigma^*_{my} = \sigma_{my} + \Delta\sigma_{dis} + \Delta\sigma_{gb} + \Delta\sigma_O + \Delta\sigma_{wh1} + \Delta\sigma_{wh2} \tag{3}$$

where $\Delta\sigma_{dis}$, $\Delta\sigma_{gb}$, $\Delta\sigma_O$, $\Delta\sigma_{wh1}$ and $\Delta\sigma_{wh2}$ are thermal expansion dislocation strengthening, small subgrain strengthening, Orowan strengthening, secondary dislocation strengthening and geometrically necessary dispersion strengthening mechanisms, respectively. They examined the mentioned microstructure strengthening mechanisms, with respect to the incremental increase in the matrix yield strength after particle incorporation. They found that the result of the combined microstructure strengthening analysis is consistent with experimental results.

The aim of this paper is the prediction of the yield strength of B_4C particle-reinforced low strength aluminum composites produced by repeated roll bonding (RRB) process. In this work, the shear lag theory modified by Sekine and Chen used for the prediction of the yield strength of the produced composites.

2. Experimental procedures

Strips of 1100-aluminum alloy with the length of 200 mm, width of 30 mm, and thickness of 0.4 mm annealed at 623 K in ambient atmosphere and the analytical grade of B_4C powder with an average size of 2.5 μm were used as the raw materials. Table 1 lists the chemical composition of the Al alloy used. The strips were degreased in acetone and scratch brushed with a 45-mm diameter stainless steel circumferential brush with 0.35 mm wire diameter. Then eight strips were stacked to achieve 3.2 mm thickness, while the B_4C powders were dispersed between each two of the layers. The stacked strips were fastened at both ends by steel wire to make it ready for the rolling process. The prepared stack of the strips was roll-bonded with a draft percentage of 66% at room temperature. The reduction of 66% was used for the creation of an appropriate bonding between the aluminum strips [10]. The well roll-bonded strip was cut into three strips by a shearing machine and annealed at 623 K in ambient atmosphere for 1 h. After the surface treatment, the three strips are stacked and then roll-bonded again, with the same reduction in thickness, while the B_4C powders was dispersed between them again. In the next step, the roll-bonded strip was cut into two strips. Then, they were annealed (at the same conditions mentioned above), degreased in acetone, scratch brushed, staked over each other, without the B_4C particles between them, and roll-bonded with a draft percentage of 50% reduction (Von Mises equivalent strain of 0.8). This step of the process was repeated up to six cycles, where after each cycle, the strips were annealed and prepared to be stacked and roll bonded again. After eight roll-bonding cycles in total (including two cycles in the first step and next six cycles in the second step of the RRB process), the Al matrix composite strip, including well-dispersed B_4C reinforcements was produced.

The roll-bonding experiments were carried out at room temperature, without lubricant, using a laboratory rolling mill with a loading capacity of 15 tons. The roll diameter was 150 mm, and the rolling speed (ω) was 15 rpm. Tensile tests at ambient temperature were carried out to have an estimate about the mechanical properties of the composite strips produced in the final roll-bonding cycles, and after annealing at an initial strain rate of $8.3 \times 10^{-4}\ s^{-1}$, by using a universal testing machine. The tensile test specimen was 10 mm in gage length and 5 mm in gage width, which is the 1/5 miniaturized size of the JIS-5 specimen. Optical microscopy (OM) was used to observe the microstructure and to investigate how well the B_4C particles have been distributed in the produced composites at final roll-bonding cycles.

3. Results and discussion

3.1. Microstructure observation

The microstructures of the 5 and 10 vol.% B_4C particulates composites produced by the RRB process in the eighth rolling cycles are shown in Figs. 1 and 2, respectively. Note that the optical microscopy was performed on the rolling direction (RD)–normal direction (ND) plane of the composites. It can be seen after the six

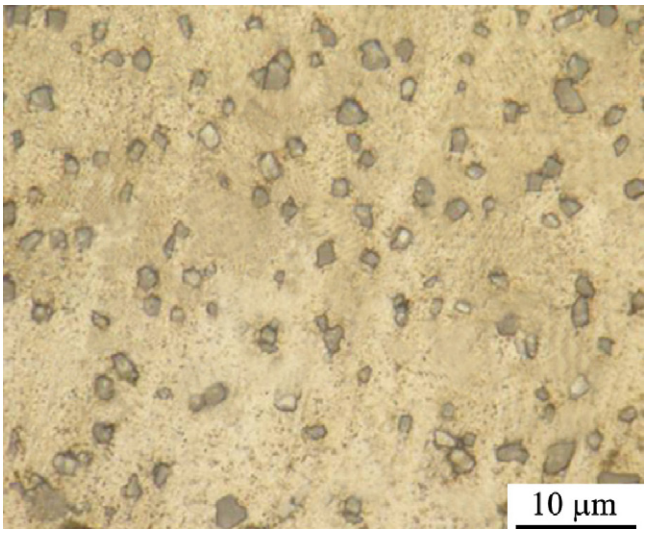

Fig. 1. OM micrographs of the Al/5 vol.% B_4C composite microstructures produced by the RRB process in the final rolling cycles.

RRB cycles, an Al matrix without porosities and cracks is obtained. However, a number of B_4C particle agglomerations and clustering can be observed in the structure. Since the agglomerations include some porosities and cracks, they are deleterious to the mechanical properties.

3.2. Mechanical properties

The stress–strain curves of the produced composites (Al/5 and 10 vol.% B_4C) after the various rolling cycles are shown in Figs. 3 and 4. It can be seen that the tensile strength increases by increasing the number of rolling cycles up to the eighth cycles. In the initial rolling cycles, bonding between the strips is weak, and it gets stronger by increasing the rolling cycles [11]. The presence of

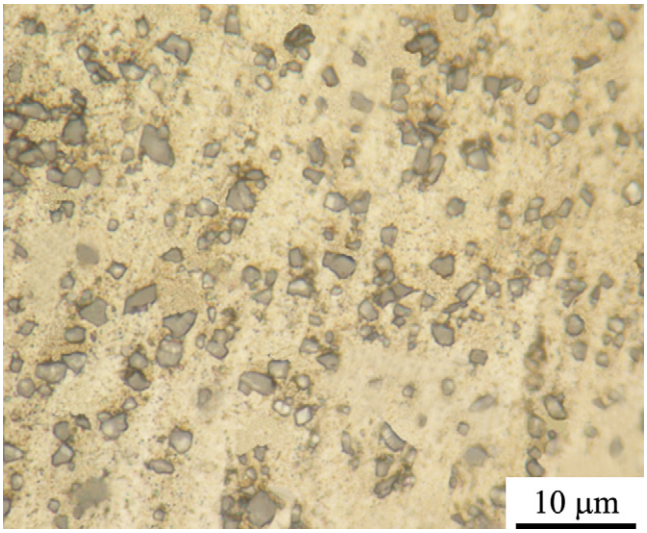

Fig. 2. OM micrographs of the Al/10 vol.% B_4C composite microstructures produced by the RRB process in the final rolling cycles.

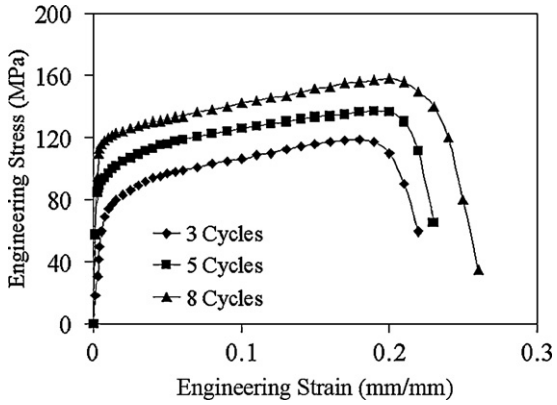

Fig. 3. Engineering stress–strain curve of the Al/5 vol.% B_4C composite produced by the RRB process in the various cycles.

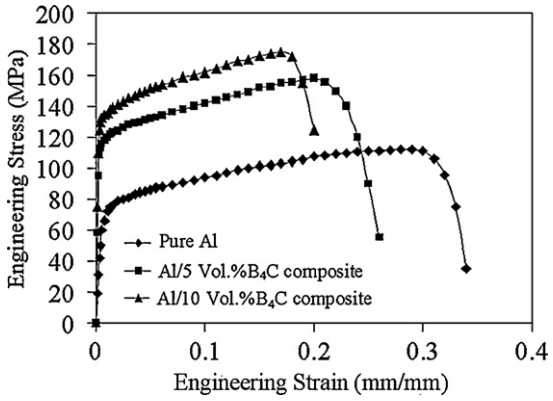

Fig. 5. Engineering stress–strain curve of the 5 and 10% composite and the pure Al (raw material).

porosities between the layers is the main reason for obtaining the lower strength in the samples which produced in the initial rolling stages [11]. By increasing the number of cycles, better bonding is created between the layers and the porosities are omitted, which results in the higher strengths. Moreover, in the initial cycles of the rolling process the work piece has a layered structure, in which the layers of the B_4C powders discrete the metal layers [11]. By increasing the number of the Al and B_4C layers in the cross-section, as a result of increasing the rolling cycles, the B_4C particles are dispersed more uniformly in the aluminum matrix; therefore, the tensile strength increases [11]. The engineering stress–strain curves of the Al/B_4C composites produced by the RRB process (after the eighth cycle of the rolling cycle) and also engineering stress–strain curves of an annealed commercial pure aluminum, as the raw material, are compared in Fig. 5. It is seen that the strength of the Al/10 vol.% B_4C composite is higher than that of the Al/5 vol.% B_4C composite: the tensile strength of the 10% composite is about 1.2 times higher than that of the 5% composite. However, the strength of both the composites is higher than that of the raw material.

3.3. Strength prediction

3.3.1. Thermal expansion dislocation strengthening

It was verified that the dislocation density in the matrix of composites is higher than that in the unreinforced matrix [3]. The large difference in thermal expansion between aluminum and B_4C particles results in the generation of dislocations on quenching from the recrystallization or solution treatment temperature [4]. The dislocation density caused by the large difference between the thermal expansion coefficients of the particles and aluminum can be calculated from the Arsenault model [12]:

$$\rho = \frac{4V_f \Delta T \Delta C}{b(1-V_f)}\left(\frac{1}{t_1}+\frac{1}{t_2}+\frac{1}{t_3}\right) \quad (4)$$

That is, the dislocation density (ρ) is a function of reinforcement size (d), Burgers vector of matrix (b), volume fraction of reinforcement (V_f), the mismatch between the thermal expansion coefficients of the particles and aluminum (ΔC), the temperature change from the heat treatment temperature of the matrix to room temperature (ΔT) and dimensions of particles with parallelepiped shape (t_1, t_2, t_3). Substituting the three dimensions $t_1 = t_2 = a$ and $t_3 = 1.5a$ into Eq. (4), where a is the average width of the particles, we obtain

$$\rho = \frac{32V_f \Delta T \Delta C}{3b(1-V_f)a} \quad (5)$$

The strength ($\Delta\sigma_{dis}$) can be estimated by an expression such as [4]:

$$\Delta\sigma_{dis} = \alpha G b \rho^{1/2} \quad (6)$$

where G and b are the shear modulus and Burgers vector of the matrix material ($b = 0.286$ nm) respectively and α is the dislocation strengthening efficiency. Sekine and Chen [3] reported that α is between 0.5 and 0.8 for pure metals, and Miller and Humphreys [4] reported that α is between 0.5 and 1 for 1050 aluminum. In this paper, the average value of this constant number (0.7) was used. Some mechanical and physical properties of the B_4C particle reinforcements and 1100 pure aluminum alloy matrix used for prediction are shown in Table 2. In the produced composites by the RRB process, the average size reinforcement (d) is 2.5 μm. The volume fraction (V_f) of the B_4C particle are two value of 5 and 10%. In addition, CTE_{Al} is $24 \times 10^{-6}\ K^{-1}$ and CTE_{B_4C} is $5 \times 10^{-6}\ K^{-1}$; therefore, ΔC is $19 \times 10^{-6}\ K^{-1}$. The shear modulus and Burgers vector of the matrix (1100 Al) are 26 GPa and 0.286 nm, respectively. From Eq. (5), ρ is equal to 7.81×10^{12} and $1.65 \times 10^{13}\ m^{-2}$ for the 5 and 10 vol.% B_4C particulates composites, respectively. From Eq. (6), $\Delta\sigma_{dis}$ can be calculated to be about 14.55 and 21.14 MPa for the 5 and 10 vol.% B_4C particulates composites, respectively. The above analysis assumes that the dislocations are uniformly distributed and all the dislocations generated can contribute to $\Delta\sigma_{dis}$ This may not be true for a solution hardened matrix [4].

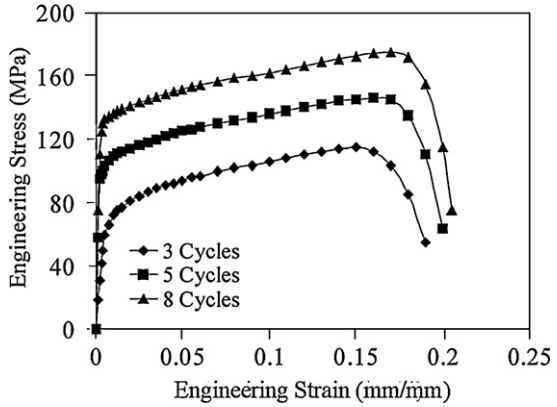

Fig. 4. Engineering stress–strain curve of the Al/10 vol.% B_4C composite produced by the RRB process in the various cycles.

3.3.2. Small subgrain strengthening

Obviously, the yield strength of a matrix with smaller grain size is larger than that with larger grain size. Recrystallization of the matrix of the composites may occur by particle-stimulated nucleation, and grain boundary movement will be impeded by the

Table 2
Some mechanical and physical properties of the B_4C particle reinforcements and 1100 pure aluminum.

Material	Young's modulus (GPa)	Shear modulus (GPa)	Poisson's ratio	Coefficient of thermal expansion ($10^{-6}\,^{\circ}C^{-1}$)	Diameter (μm)
1100 Aluminum	68.9	26	0.33	24	–
B_4C	460	184	0.17	5–5.6	2.5

existence of the particles. As a result, the grain size in the matrix becomes smaller than that in the unreinforced alloys [3]. If it is assumed that each particle nucleates one grain, the resultant grain size D can be expressed by [4]:

$$D = d\left[\frac{1 - V_f}{V_f}\right]^{1/3} \tag{7}$$

where d is the average diameter of the particles. The incremental increase of the yield strength $\Delta\sigma_{dis}$ of the matrix due to the smaller grain size can be estimated from the Hall–Petch equation, as follows [4]:

$$\Delta\sigma_{gb} = \left[\frac{K_y}{D}\right]^{1/2} \tag{8}$$

where K_y is a constant and is typically equal to 0.1 MN $m^{-3/2}$ for aluminum. As it can be seen from Eqs. (7) and (8), the yield strength increment due to the small grain size can be obtained as a function of the particle volume fraction. In the present work, D is about 6.7 and 5.2 μm (from Eq. (7)) for the 5 and 10 vol.% B_4C particulates composites, respectively. Therefore, from Eq. (8), $\Delta\sigma_{gb}$ is 38.6 and 43.85 MPa for the 5 and 10 vol.% B_4C particulates composites, respectively.

3.3.3. Orowan strengthening

The Orowan bypassing of particles by dislocations can increase materials strength. If the particles are assumed to be equiaxed then the strengthening (σ_o) is estimated to be [13]:

$$\Delta\sigma_O = \frac{2Gb}{L}$$

$$L = 6d\left(\frac{2\pi}{V_f}\right)^{1/2} \tag{9}$$

where L is the interparticle spacing. This term σ_o is negligible unless for particles smaller than 1 micron are considered. However, as in this work the average B_4C particles size is 2.5 μm and the volume percent of them in low (the interparticle spacing is high), σ_o is zero approximately.

3.3.4. Secondary dislocation strengthening

Dislocations may be produced at the interfaces of particles when the composite is deformed. Since the particles are not deformed and the interfaces between the particles and matrix are not fractured, secondary slip must occur locally around each particle when the matrix is deformed. The density of secondary dislocations rises steeply with the increase of strain, and acts as a forest to impede the movement of the primary glide dislocations. The increment of tensile stress due to this mechanism is as follows [3,4]:

$$\Delta\sigma_{wh1} = KG\left(\frac{V_f b}{d}\right)^{1/2}\varepsilon^{1/2} \tag{10}$$

where K is a constant and ε is the tensile strain. The reasonable value of the constant K is between 0.2 and 0.4, which shows the degree of secondary dislocations to obstruct the movement of primary ones [3]. In this study, the value of K is taken as 0.3 and the tensile strain ε is taken as the matrix yield strain, 0.002. Therefore, the $\Delta\sigma_{wh1}$ value is 0.83 and 1.18 MPa for the 5 and 10 vol.% B_4C particulates composites respectively, which are negligible. Also from Eq. (10), we can predict the incremental increase of the matrix yield strength due to this mechanism as a function of the particle volume fraction.

3.3.5. Geometrically necessary dispersion strengthening

Geometrically necessary dislocations are formed in the matrix in the condition of tensile stress. When the particulates metal matrix composites are loaded, the particles are deformed less than the matrix, or not at all, so that gradients of deformation are formed in the matrix. Dislocations are stored in the matrix to accommodate the deformation gradients and allow the compatible deformation of particles and matrix [14]. When the dislocation array required for compatible deformation is considered as a prismatic array, the increment of the average principal stress at the particle surface is obtained as follows [3,15]:

$$\Delta\sigma_{wh2} = \frac{2G(1-\nu)}{(1-2\nu)}V_f\varepsilon \tag{11}$$

where ν is the matrix Poisson's ratio. When the tensile strain is taken as the aluminum matrix yield strain of 0.002, the increment of the yield strength of the matrix due to this mechanism for the composites produced in this study is 10.25 and 20.5 MPa.

Table 3 tabulates the values of $\Delta\sigma_{dis}$, $\Delta\sigma_{gb}$, $\Delta\sigma_O$, $\Delta\sigma_{wh1}$, $\Delta\sigma_{wh2}$, σ_{my} and σ^*_{my} for the composites produced in this study. As it can be seen, the value of σ^*_{my} in the 10% composite is higher than that in the 5% composite.

As mentioned above, to predict the yield strength of the Al/B_4C composites produced by the RRB process, the method reported by Sekine and Chen [3] was used. In the calculations, the average diameter of the particles was set at 2.5 μm, and the particle volume fractions were 5 and 10%. The mean aspect ratio of the B_4C particles used in this work was measured about 1.5. Note that to determine the mean aspect ratio, at least 50 particles were randomly considered via scanning electron microscopy observations. By substituting the increments of the yield strength calculated by the mentioned mechanisms and the values of S, V_f and V_m into Eq. (3), the predicted yield strength of the Al/B_4C composite is given. The yield strength calculated by this model and measured by the tensile test on the composite produced by the RRB process is listed in Table 4. As it can be seen, there is an agreement between the calculated and experimental yield strengths. The difference between the calculated and experimental values can be regarded form two viewpoints. At first, it should be considered that the different microstructure strengthening mechanisms interact with each other and the increments of the yield strength

Table 3
Values of the increment yield strength of the matrix.

Property (MPa)	V_f (%)	
	5	10
Yield strength of the matrix without the B4C particles (σ_{my})	62	62
Thermal expansion dislocation strengthening ($\Delta\sigma_{dis}$)	14.55	21.14
Small subgrain strengthening ($\Delta\sigma_{gb}$)	38.6	43.85
Orowan strengthening ($\Delta\sigma_o$)	0	0
Secondary dislocation strengthening ($\Delta\sigma_{wh1}$)	0.8	1.13
Geometrically necessary dispersion strengthening ($\Delta\sigma_{wh2}$)	10.25	20.5
σ_{my}	126.2	148.62

Table 4
Experimental and predicted results of the yield strength of the Al/B_4C composites produced by the RRB process.

Yield strength (MPa)	V_f (%)	
	5	10
Calculated by Sekine's model	130.93	159.76
Experimental by the tensile test	117.5	133.8

may not be added linearly. Secondly, some kinds of defects in the Al/B_4C composites, such as voids, non-uniform particle distribution, inadequate bonding between the Al layers and particularly B_4C agglomerations will decrease the yield strength of the composites, which was not considered in the calculations. As mentioned in Section 3.1, there are some B_4C agglomerations in the both produced composite.

As seen in Figs. 1 and 2, the number of agglomerations in the 10 vol.% B_4C particulates composite is more than that in 5 vol.% B_4C particulates composite. According to literature [16], the increase in the fraction of reinforcement particles increases agglomeration and consequently the amount of porosities in composites. Therefore, it is expected that the fraction of porosities in the 10 vol.% B_4C particulates composite is more than that in the 5 vol.% B_4C particulates composite. This fact explains the difference between the experimental and calculated yield strength listed in Table 4, where the difference for the 10 vol.% B_4C particulates composite is more than the 5 vol.% B_4C particulates composite.

4. Conclusions

In this study, Al/5 and 10 vol.% B_4C composites were produced in the form of sheets through RRB process successfully. The microstructure of the composites were investigated by OM. Furthermore, the yield strength of the produced composite samples was measured by tensile tests and compared with values calculated via theoretical strength analysis based on Sekine's model. The conclusions drawn from the results can be summarized as follows:

1. The OM microstructures revealed the well distributed B_4C particles in the aluminum matrix for both the composites.
2. The tensile strength of the Al/10 vol.% B_4C composite is higher than that of the Al/5 vol.% B_4C composite.
3. There is a good agreement between the calculated yield strength and experimental value for both the composites.
4. The difference between the calculated and experimental values is due to some defects.
5. The Orowan strengthening mechanism has no significant effect on the yield strength of the composite produced in this work, because the average B_4C particles size is higher than 1 μm.

Acknowledgement

The author would like to thank Shiraz University due to the support for this study.

References

[1] J.W. Kaczmar, K. Pietrzak, W. Wlosinski, J. Mater. Process. Technol. 106 (2000) 58–67.
[2] H.Y. Wang, Q.C. Jiang, Y. Wang, B.X. Ma, F. Zhao, Mater. Lett. 58 (2004) 3509–3513.
[3] H. Sekine, R. Chen, Composites 26 (1995) 183–188.
[4] W.S. Miller, F.J. Humphreys, Scripta Metall. Mater. 25 (1991) 33–38.
[5] H.L. Cox, Br. J. Appl. Phys. 3 (1952) 72–79.
[6] V.C. Nardone, K.M. Prewo, Scripta Metall. 20 (1986) 43–48.
[7] V.M. Karbhari, D.J. Wilkins, Scripta Metall. Mater. 25 (1991) 707–712.
[8] R.J. Arsenault, Mater. Sci. Eng. 64 (1984) 171–181.
[9] M. Taya, K.E. Lulay, D.J. Lloyd, Acta Metall. Mater. 39 (1991) 73–87.
[10] M. Alizadeh, M.H. Paydar, Mater. Des. 30 (2009) 82–86.
[11] M. Alizadeh, M.H. Paydar, J. Alloys Compd. 477 (2009) 811–816.
[12] R.J. Arsenault, N. Shi, Mater. Sci. Eng. 81 (1986) 175–187.
[13] G.E. Daibin, G.U. Mingyuan, Mater. Lett. 49 (2001) 334–339.
[14] M. Alizadeh, M.H. Paydar, J. Alloys Compd. 492 (2010) 231–235.
[15] M.F. Ashby, Philos. Mag. 21 (1970) 399–424.
[16] M. Kok, J. Mate, Process Technol. 161 (2005) 381–387.